Living Along COVID-19: Assessing Contention Policies Through Agent-Based Models

Daniele Baccega[1,2(✉)], Simone Pernice[1,2], Paolo Castagno[1], Matteo Sereno[1,3], and Marco Beccuti[1,2,3]

[1] Computer Science Department, Universitá di Torino, 10149 Turin, Italy
daniele.baccega@unito.it
[2] Laboratorio InfoLife, Consorzio Interuniversitario Nazionale per l'Informatica (CINI), Rome, Italy
[3] Competence Centre for Scientific Computing C3S, Universitá di Torino, 10124 Turin, Italy

Abstract. SARS-CoV-2 has become an endemic disease, and we will have to face the continuous rise of new variants. Designing and evaluating the effects of new containment policies is of primary importance to keep social activities going as safely as possible according to the different stages of the pandemic. Therefore, we propose an Agent-Based Model to study the evolution of SARS-CoV-2 spread in a well-defined environment (of small/medium size, like a shop, a restaurant, an office, a school, with fewer than a hundred or a few hundred people) to assess the efficacy of different non-pharmaceutical interventions and vaccination strategies. Specifically, we focused on schools, given that the COVID-19 quarantine has resulted in substantial disruptions to education, leading to a transition to remote learning and worsening educational inequalities. We consider using face masks and several real-world testing protocols combined with quarantine policies. All protocols/policies have been evaluated at various stages of the pandemic evolution. Results show that testing campaigns are effective as far as the testing process is faster than the virus diffusion. Also, vaccination campaigns covering less than 40% of the susceptible population provide poor results in protecting from a major outbreak, even if the circulation of the virus is low. Our empirical findings reveal a decreasing effectiveness of various policy implementations as viral circulation intensifies. Additionally, our analysis shows a consistent reduction in infection rates due to the continued use of facial protective measures, regardless of the level of viral circulation.

Keywords: Agent-Based Simulation · Non-Pharmaceutical Interventions · COVID-19 · School

1 Introduction

The COVID-19 pandemic highlighted the difficulties in managing a worldwide emergency. One of the primary challenges has been keeping people safe

M. Vettoretti et al. (Eds.): CIBB 2023, LNBI 14513, pp. 143–161, 2025.
https://doi.org/10.1007/978-3-031-90714-2_11

while doing their normal activities, such as going to school. Different non-pharmaceutical interventions (NPIs)—such as distancing requirements, masks, rooms' air ventilation, screening, and quarantine—were used to control the spread and to avoid the collapse of often fragile and overloaded healthcare systems. In addition, the onset of new SARS-CoV-2 variants, such as the Omicron variant, exhibited a high degree of immune evasion, leading to increased infection rates worldwide [1]. The advent of vaccines has significantly contributed to reducing the number of deaths [2]. However, in the school setting, children were not initially covered by the vaccine, and even after that, their vaccine coverage grew slowly.

The efficacy of NPIs was studied using different types of modeling [3]: Susceptible-Exposed-Infected-Recovered-Susceptible (SEIRS) compartmental model [4], aerosol transmission model [5–7], Agent-Based Models [8–14]. In this work, we propose an extension of the Agent-Based Model developed in [15] to study the spread of SARS-CoV-2 infections within an explanatory scholastic environment (see Fig. 1) and to analyze different intervention strategies to provide policymakers valuable insight to face future emergencies.

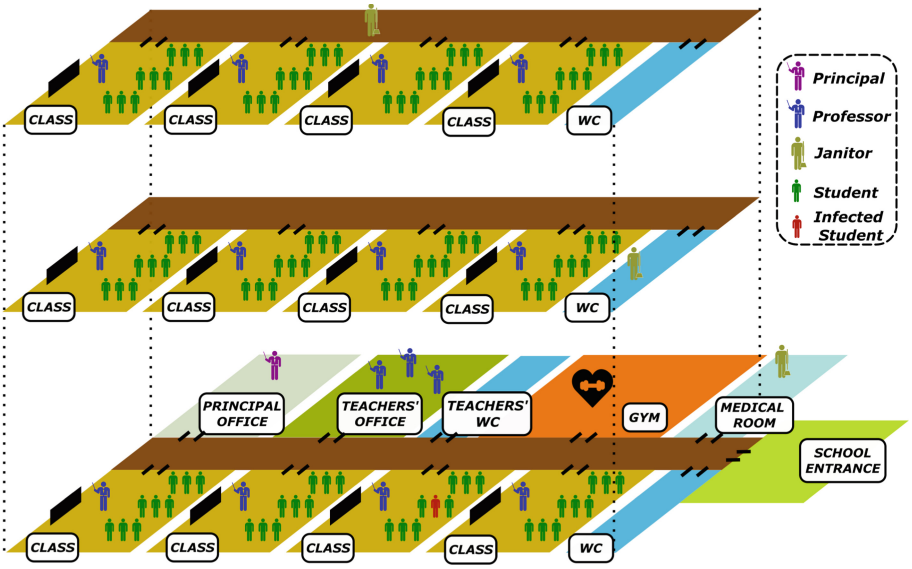

Fig. 1. Graphical representation of a generic school featuring 12 classrooms distributed across three floors, along with common areas such as the entrance, corridors, bathrooms, stairs, gym, medical room, teachers' office, and principal's office. Each classroom includes twenty-four desks, evenly spaced apart, along with a teacher's desk and a blackboard at the front. The school population consists of a total of 290 individuals, including 240 students, 49 teachers, and a principal [15].

2 Data and Methods

Agent-Based Models (ABMs) simulate complex systems by representing individual entities, or agents, each with specific rules and behaviors. These agents interact with one another and their environment, leading to the emergence of system-level patterns and dynamics. ABMs allow modelers for a nuanced exploration of the intricate relationships and behaviors that shape complex systems.

This work proposes an ABM, developed in the multi-agent programmable modeling environment NetLogo version 6.1.1 [16], that compounds *i)* a detailed description of the environment and the population dynamics within such environment—including both how agents move within the physical spaces and social contact structure of the population—, *ii)* the COVID-19 progression model—modeled as a Susceptible-Exposed-Infected-Recovered (SEIR) compartmental model—, and *iii)* the non-pharmaceutical interventions (NPIs) available to contain the infection spreading.

As an example scenario, graphically depicted in Fig. 1, we considered a school with 12 classrooms (arranged on three floors) with shared spaces (i.e., entrance, corridors, bathrooms, stairs, gym, medical room, teachers' office, and principal's office). Each floor consisted of one corridor connecting all the rooms and one bathroom only for students. The school entrance, the gym, the medical room, the teacher's office, the principal's office, and the teachers' bathroom are all on the first floor. Each classroom is characterized by twenty-four desks (equally distanced from each other), one teacher's desk, and a blackboard. Students and personnel—overall 290 people divided into 240 students, 49 teachers, and a principal—move across the school according to their role and schedule (e.g., students stay in classrooms and at most they can go to the bathroom during classes, and teachers are allowed to move across the school during class changes). Students' schedules foresee 30 classes of 50 min each, from Monday to Friday. Students arrive at school from 7:35 a.m., with the first class beginning at 8:10 a.m. A school day consists of six classes of 50 min each and two breaks. The first break is between the second and the third classes, while the second one is after the fourth class. At the beginning of each simulation students are allocated to classrooms (i.e., the first twenty agents are allocated to one classroom, and so on), and this association lasts for the whole simulation. Teachers move from one classroom to another according to their schedules.

The COVID-19 progression model is a Susceptible-Exposed-Infected-Recovered (SEIR) model (showed in Fig. 2) where the population is divided into four compartments: *i)* the Susceptible (S) population consists of healthy individuals who have not yet been exposed to the disease, *ii)* the Exposed (E) population includes those who have been exposed and are infected, but are not yet infectious, *iii)* the Infected (I) population comprises individuals who can transmit the disease to others, and *iv)* the Recovered (R) population includes those who have recovered from the disease. Each agent is labeled with a specific disease progression status, whose parameters are reported in Table 2. In particular, we labeled each agent with one of the four statuses of the disease progression, updating it as follows: *i)* from the susceptible status to the exposed one—to

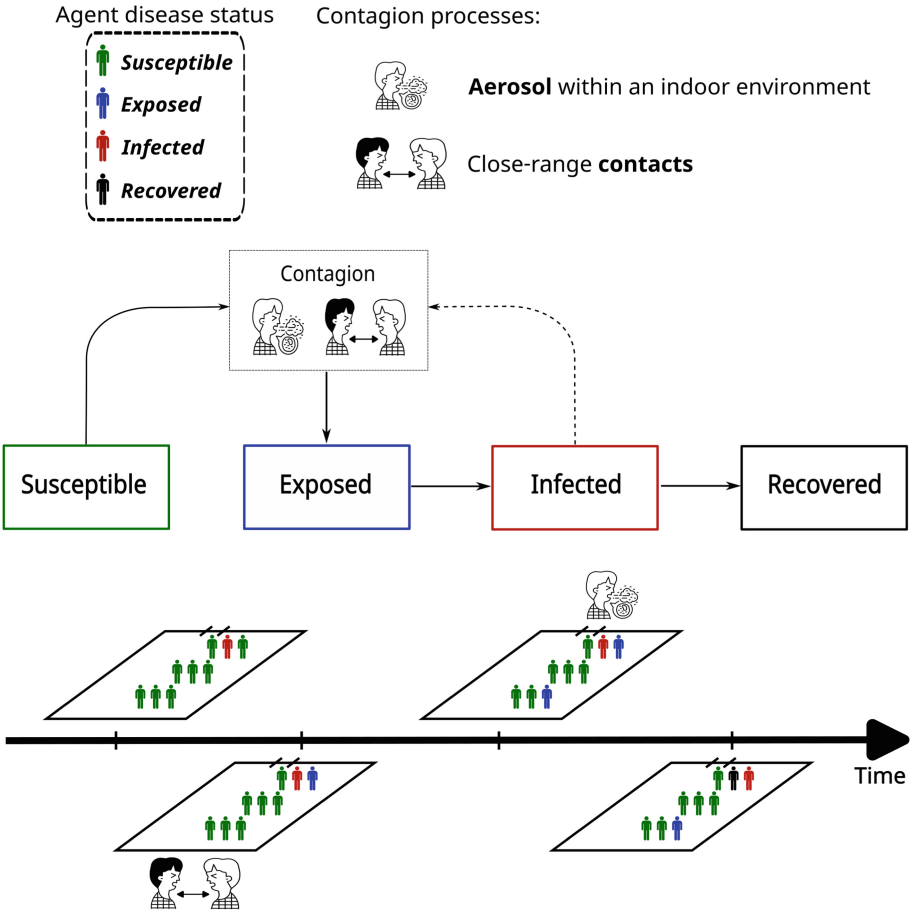

Fig. 2. The COVID-19 progression model (SEIR)—the dashed line indicates that contagion occurs via close-range contacts with an infected individual [17] or through aerosol transmission [7]—with an example of its evolution. We considered four time points: t_1, t_2, t_3, and t_4 ($t_1 < t_2 < t_3 < t_4$). At time t_1, all agents are susceptible except one infected. By time t_2, a nearby agent becomes exposed due to close-range transmission. At time t_3, a distant agent becomes exposed via aerosol transmission. Finally, at time t_4, the initially infected agent recovers, the close-range contact exposed agent becomes infected, and the aerosol-exposed agent remains exposed.

model the virus exposure—, *ii)* from the exposed status to the infected one—when the incubation period ends, and agents become contagious—, *iii)* from the infected status to the recovered one—when the infectious period ends.. The virus exposure is modeled through two different drivers: either close-range contacts [17] between susceptible and infected agents or through aerosol [7] within an indoor environment.

In the former case, the probability of successful contagious contact is associated with each susceptible agent (S_i) that remains within an area ($\mathbf{A}$) of 4.41 m^2 surrounding an infected agent. This probability is determined by the following function [17]:

$$P_{S_i} = c_r \frac{C_{S_i}}{\mathbf{A}} \tag{1}$$

where c_r represents the *contamination risk*, and C_{S_i} denotes the total time (in minutes) that the S_i agent remains within the vicinity of an infected agent.

In contrast, the spread of the pathogen via aerosol is calculated based on the *quanta* concentration in each room. A quanta is defined as the dose of airborne droplet nuclei necessary to infect 63% of susceptible individuals [18]. Following the approach in [7], we determine the number of quanta inhaled by each agent in a given room (e.g., classrooms, bathrooms, etc.) to compute the probability of infection without direct contact with an infected agent. This probability is given by the following function:

$$P_{S_i} = 1 - e^{-\frac{N_{\text{virus}}}{k_p}} \tag{2}$$

where k_p represents the reciprocal of the probability that a single pathogen particle will trigger an infection [7,19], and N_{virus} denotes the number of quanta inhaled by each susceptible agent during a time interval Δt. This value is determined by solving the following differential equation:

$$dN_{virus} = (1 - \eta_{mask} f_{\text{mask}})\ C(t) Q_{inh}\ dt \tag{3}$$

where η_{mask} is the efficacy of the masks, f_{mask} represents the proportion of agents correctly wearing a mask, $C(t)$ denotes the quanta concentration at time t, and Q_{inh} is the inhalation rate. Observe that quanta concentration at time t mainly depends on the number of people within a room, the number of infections, and the room's ventilation.

In Fig. 2, we illustrate an example of the transitions between different statuses over four time points: t_1, t_2, t_3, and t_4 ($t_1 < t_2 < t_3 < t_4$). At time t_1, all agents in the room are susceptible, except for one infected. At time t_2, an agent close to the infected agent becomes exposed due to close-range transmission [17]. At time t_3, another agent, located further away from the initially infected individual, becomes exposed through the aerosol transmission [7]. Finally, at time t_4, the initially infected agent has recovered, the agent previously exposed at close-range transmission has become infected, and the agent exposed through aerosol transmission remains exposed.

Eventually, several NPI policies can be implemented to prevent the infection from spreading within the school. A contention policy might require the application of one or more NPIs, compounding both actions aimed at reducing contact between students and their exposure to the infection. In particular, the considered NPIs are distancing requirements, rooms' air ventilation, masks, quarantine, and testing campaigns. As a baseline for all the experiments, we assumed that

desks are equally distanced from each other, and if masks are required, students use them correctly and for all the time they are at school. Likewise, the ventilation process to replace contaminated with clean air is carried out constantly at 3 Air Changes per Hour (ACH).

Several modifications to the model presented in [15] were introduced to study the efficacy of different contention policies. First, the arising of new variants required to take into account in the model the presence of several pathogens, with different infection characterizations—namely Alpha, Beta, Delta, Omicron BA.1, and Omicron BA.2 variants were introduced. In particular, COVID-19 variants are versions of the SARS-CoV-2 virus with specific genetic mutations. Some variants may exhibit changes in transmissibility, severity, and resistance to immunity. We used the results of [20] to adjust the transmissibility of the selected variant. Furthermore, to account for interactions with the environment outside the school, we considered external screening campaigns and infections due to personal interactions in other environments, such as at home. In particular, two different probabilities of external screening are applied to students every day: the probability of testing a student due to sporting activities that involve screening campaigns (e.g., playing soccer) and the probability of testing a student outside the school due to the presence of some symptoms.

The efficacy of a given contention policy strongly depends on the virus circulation. Modeling the prevalence of the infection in the general population and reflecting it on the spreading dynamics within the school required further modifications. Specifically, the model must account for the fact that any student will likely catch the infection outside the school. Therefore, we introduced the infection outside the school as a stochastic arrival process, so that the intensity of people getting the infection outside the school reflects the infection's prevalence in the population. In particular, a probability is applied to each susceptible agent every day, representing the possibility of infection outside the school (see Table 2).

3 Results

For studying the efficacy of NPIs and vaccination policies in schools, we considered both active and passive interventions: the former requires actions from the healthcare system, while the latter only requires the students to behave according to some specific indications. The active interventions consist of vaccinations and testing campaigns. While we considered as passive interventions social distancing as a common baseline behavior, rooms' air ventilation, and using masks—surgical or FFP2—and quarantine as possible contention policies.

In all scenarios, the principal and all teachers are vaccinated. We considered two screening policies, three quarantine policies, three mask policies, four levels of vaccine efficacy (100%, 70%, 50%, and 30%), four levels of student vaccination coverage (70%, 40%, 10%, and 0%), and three levels of virus circulation (low, medium, and high). Table 1 summarizes the analyzed scenarios, with 32 scenarios for each combination of students' vaccination coverage and virus circulation levels, resulting in a total of 384 scenarios. Specifically, we define vaccine efficacy as the fraction of the vaccinated population that is effectively immune to

infection, while the remaining portion remains susceptible despite having been vaccinated. To react to the circulation of infection within the school, we considered two alternative screening policies: *i) none (NN)* where no screening policy is performed, and *ii) round robin (RR)* where the students in each classroom are divided into groups, ensuring that over a month, every student is tested, with one group being tested each week [21].

Once the infection has been discovered, three actions were considered: *no quarantine (NQ)*, *class quarantine (CQ)*, or *student quarantine (SQ)*. Specifically, NQ does not trigger any intervention when new infections are discovered, while CQ sparks a class quarantine only when the virus circulation within the classroom is over a threshold n_q, and *SQ* sparks the quarantine of single infected students when we discover them. CQ and SQ are the quarantine policies used in the Piedmont Region in November/December 2021 [22] and January/February 2022, respectively. Specifically, an infected student in quarantine does not contribute to the infection spreading. Thus, using the CQ policy, if one or more infections are detected in a given classroom, the entire class is tested. The entire classroom goes into quarantine if the total number of infections reaches or exceeds n_q. If the threshold is not met, only the infected students are quarantined, while the remaining students are retested after d_{test} days, following the same quarantine procedure described earlier. Eventually, we considered three cases for the use of masks: *i) no masks (NM)* where masks are not required, *ii) FFP2 when required (FWR)* and *iii) always on (AO)* requiring to wear no masks and surgical masks, respectively. If n_m infections are detected in a classroom, these two policies mandate the use of FFP2 masks by all students and teachers in that classroom for d_{ffp2} days.

Specifically, we considered eight clusters of results for each combination of vaccine efficacy, students vaccination coverage, and virus circulation levels (see Table 1): *i)* scenarios 1 to 4 represent our baseline, modeling a policy in which NPIs countermeasures are not implemented, *ii)* scenarios 5 to 8 account for screening policy RR and quarantine policy CQ, *iii)* scenarios 9 to 12 for quarantine policy CQ alone, *iv)* scenarios 13 to 16 for quarantine policy SQ alone, *v)* scenarios 17 to 20 for mask policy FWR and quarantine policy CQ, *vi)* scenarios 21 to 24 for mask policy FWR and quarantine policy SQ, *vii)* scenarios 25 to 28 for mask policy AO and quarantine policy CQ, and *viii)* scenarios 29 to 32 for mask policy AO and quarantine policy SQ.

Figures 3, 4 and 5 show the cumulative distribution function (CDF) of the total number of infected agents at the final time for different vaccine efficacy—decreasing moving from left to right—, several levels of students vaccination coverage—decreasing moving from top to bottom—and different NPIs combinations.

Table 1. Summary of the scenarios simulated for each students vaccination coverage (70%, 40%, 10% and 0%) and circulation level (low, medium and high).

	Quarantine Policy			Screening Policy		Mask policy			Vaccination Effectiveness			
	NQ	*CQ*	*SQ*	*NN*	*RR*	*NM*	*FWR*	*AO*	30%	50%	70%	100%
1	×			×		×			×			
2	×			×		×				×		
3	×			×		×					×	
4	×			×		×						×
5		×			×	×			×			
6		×			×	×				×		
7		×			×	×					×	
8		×			×	×						×
9		×		×		×			×			
10		×		×		×				×		
11		×		×		×					×	
12		×		×		×						×
13			×	×		×			×			
14			×	×		×				×		
15			×	×		×					×	
16			×	×		×						×
17		×		×			×		×			
18		×		×			×			×		
19		×		×			×				×	
20		×		×			×					×
21			×	×			×		×			
22			×	×			×			×		
23			×	×			×				×	
24			×	×			×					×
25		×		×				×	×			
26		×		×				×		×		
27		×		×				×			×	
28		×		×				×				×
29			×	×				×	×			
30			×	×				×		×		
31			×	×				×			×	
32			×	×				×				×

Figure 3 shows the results obtained under a low virus circulation level. The first setting shows the baseline (quarantine NQ, screening NN, mask policy NM) and allows us to understand the effect of the vaccination alone. In the case of 100% vaccine efficacy, increasing the fraction of vaccinated students reduces the probability of encountering a high number of infected agents after 60 days. As expected, decreasing the vaccine efficacy increases the probability of a higher number of infected agents. Comparing this initial setting with the second one, we observe that the introduction of screening and quarantine policies (quarantine CQ, screening RR, mask policy NM) leads to a reduction in the probability of having a higher number of infections after 60 days. Also, it can be noted that vaccination campaigns covering less than 40% of the population provide poor results in terms of number of infections. It is important to notice that the most relevant results are obtained with higher vaccine efficacy: the testing process gets less effective as infections become more likely to happen, meaning that the virus spreads faster than the pace at which testing is performed.

Table 2. Model parameters.

Parameter	Value
Number of classrooms	12
Students per classroom	20
Initial infected	0
Vaccine efficacy	100 / 70 / 50 / 30%
Students vaccination coverage	70 / 40 / 10 / 0%
Average number of days of incubation [23,24]	3
Average number of days of infection [25]	7
Duration of quarantine in days [22]	10
Virus variant	Omicron BA.1
Ventilation	3 ACH
Mask efficacy [20]	59% (surgical) / 90% (FFP2)
Mask policy	NM / FWR / AO
Quarantine policy [22]	NQ / CQ / SQ
Screening adhesion	100%
Screening policy [21]	NN / RR
Fraction of population wearing mask	100%
Probability of going to the bathroom (per minute)	$8e^{-4}$
Probability of going to the blackboard (per minute)	$6e^{-4}$
Probability of going to the principal office (per minute)	$1.4e^{-4}$
Probability of going into the hall during interval	0.532
First probability of external screening (per day)	0.0075
Second probability of external screening (per day)	0.03
Probability of outside contagion	0.0004 (low circulation) / 0.008 (medium circulation) / 0.02 (high circulation)
Contamination risk (c_r) [17]	0.024
d_{test} [22] (Section 3)	5
d_{ffp2} (Section 3)	10
n_q [22] (Section 3)	5
n_m (Section 3)	1 (FWR) / 5 (AO)
Duration of the lessons in minutes	50
Simulated days for each run	60
Number of runs for each scenario	500

The last six settings illustrate the effects of the NM, FWR, and AO mask policies in combination with CQ and SQ quarantine policies, along with NN screening. Comparing the second setting to the third one (quarantine CQ, screening NN, mask policy NM) is clear that the screening RR has a negligible impact for the used quarantine policy. Focusing the attention on quarantine policies, we can state that CQ works much better than SQ, especially in the settings with FWR and AO mask policies. Regarding mask policies, we can conclude that the AO mask policy gives the best results (especially combined with the CQ quarantine policy). This is because the AO mask policy provides a boost in the protection of about 50% by forcing the use of FFP2 masks—see Table 2. In addition, opposite to what happens in the case of testing, the impact of the AO mask policy increases as the vaccine efficacy decreases. Indeed, despite how fast the infection spreads, masks always provide the same level of protection.

Figures 4 and 5 show the same eight settings under a medium and high virus circulation level. Once again, we find that increasing the fraction of vaccinated students reduces the probability of observing a high number of infected agents after 60 days while decreasing vaccine efficacy increases this probability. These results indicate that containing the spread is more challenging under medium and high virus circulation levels compared to low virus circulation level. However, a combination of masks and quarantine policies can effectively reduce the final number of infected agents. Moreover, Fig. 6 displays the area under the CDF (normalized between 0 and 1) for each scenario, making it easier to compare the effects across different levels of virus circulation.

Figures 7, 8 and 9 illustrate the distribution of infections over time and the average number of infections. Representing the evolution of the infection distribution allows us to understand how interventions contribute to containing the

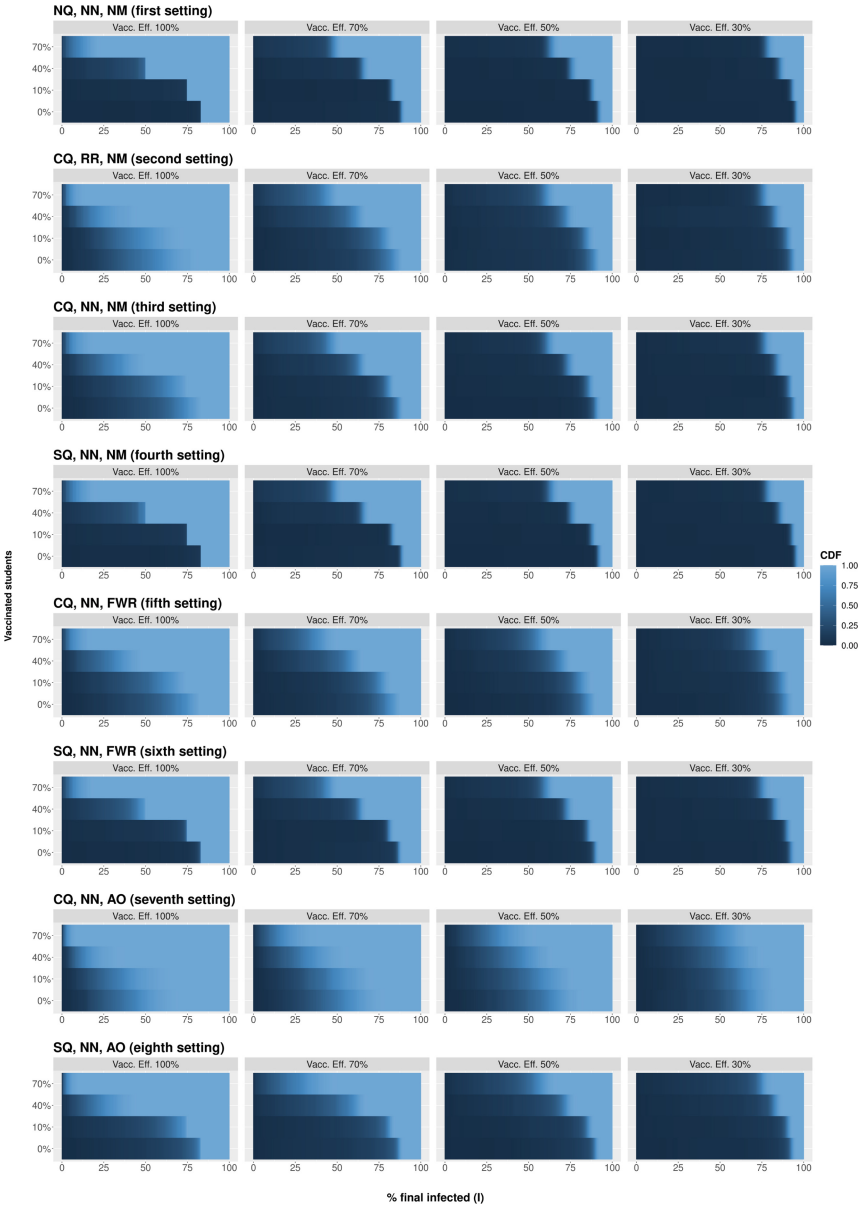

Fig. 3. Cumulative distribution function (CDF) of the total number of infected agents at the final time for each considered scenario under a low virus circulation level. For each scenario—identified by the setting (on the rows), the vaccine efficacy (on the columns), and the fraction of vaccinated students (on the rows of each subplot)—we run 500 simulations—see Table 2. Lighter CDFs indicate more effective countermeasures. The first, second, and seventh settings are the most noteworthy. The first setting (NQ, NN, NM) shows that higher infections are associated with lower vaccine efficacies and lower fractions of vaccinated students. The second setting (CQ, RR, NM) shows that a fraction of vaccinated students $< 40\%$ provides poor results in terms of levels of protection—the testing process gets less effective as infections become more likely to happen. Finally, the seventh setting (CQ, NN, AO) shows that masks are more effective with lower vaccine efficacies—masks always provide the same level of protection.

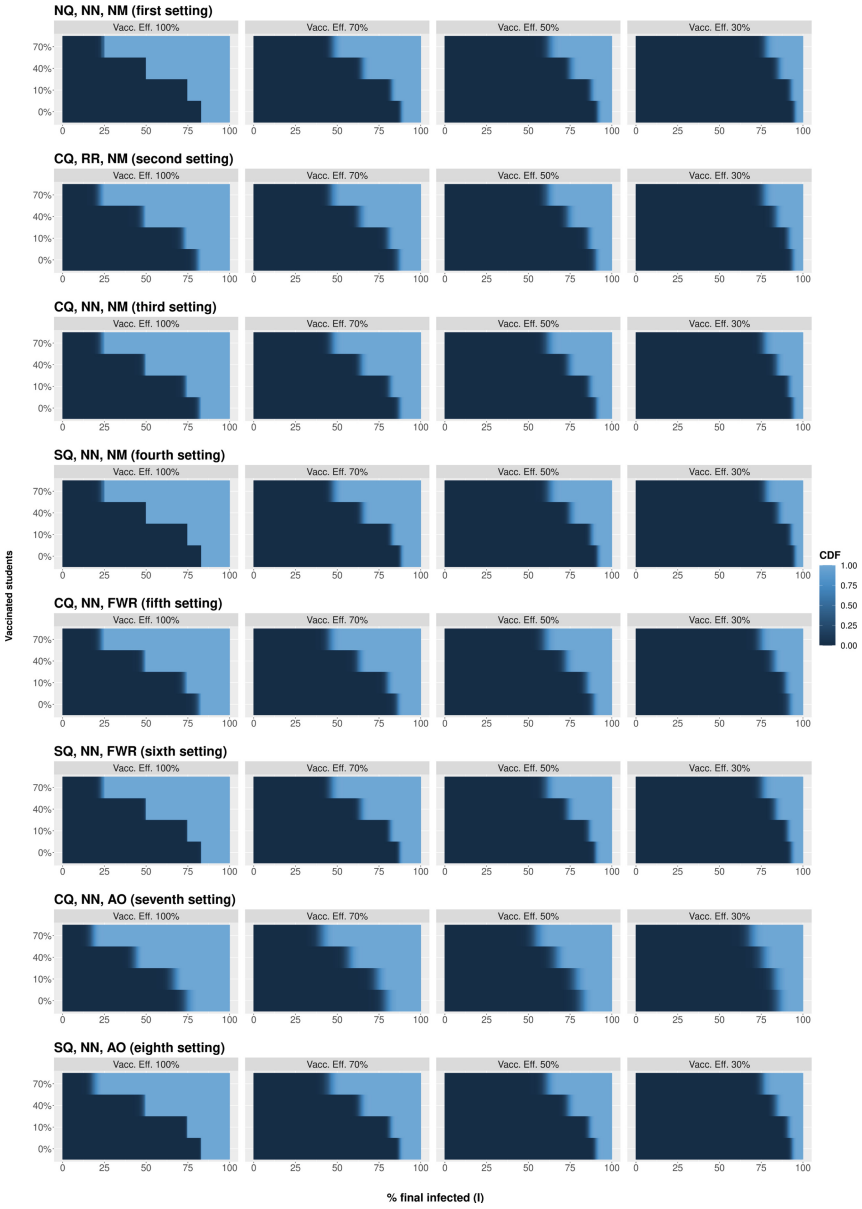

Fig. 4. Cumulative distribution function (CDF) of the total number of infected agents at the final time for each considered scenario under a medium virus circulation level. For each scenario—identified by the setting (on the rows), the vaccine efficacy (on the columns), and the fraction of vaccinated students (on the rows of each subplot)—we run 500 simulations—see Table 2. Lighter CDFs indicate more effective countermeasures. We can state that higher infections are associated with lower vaccine efficacies and lower fractions of vaccinated students and a combination of masks and quarantine policies allows to reduce the final number of infected agents.

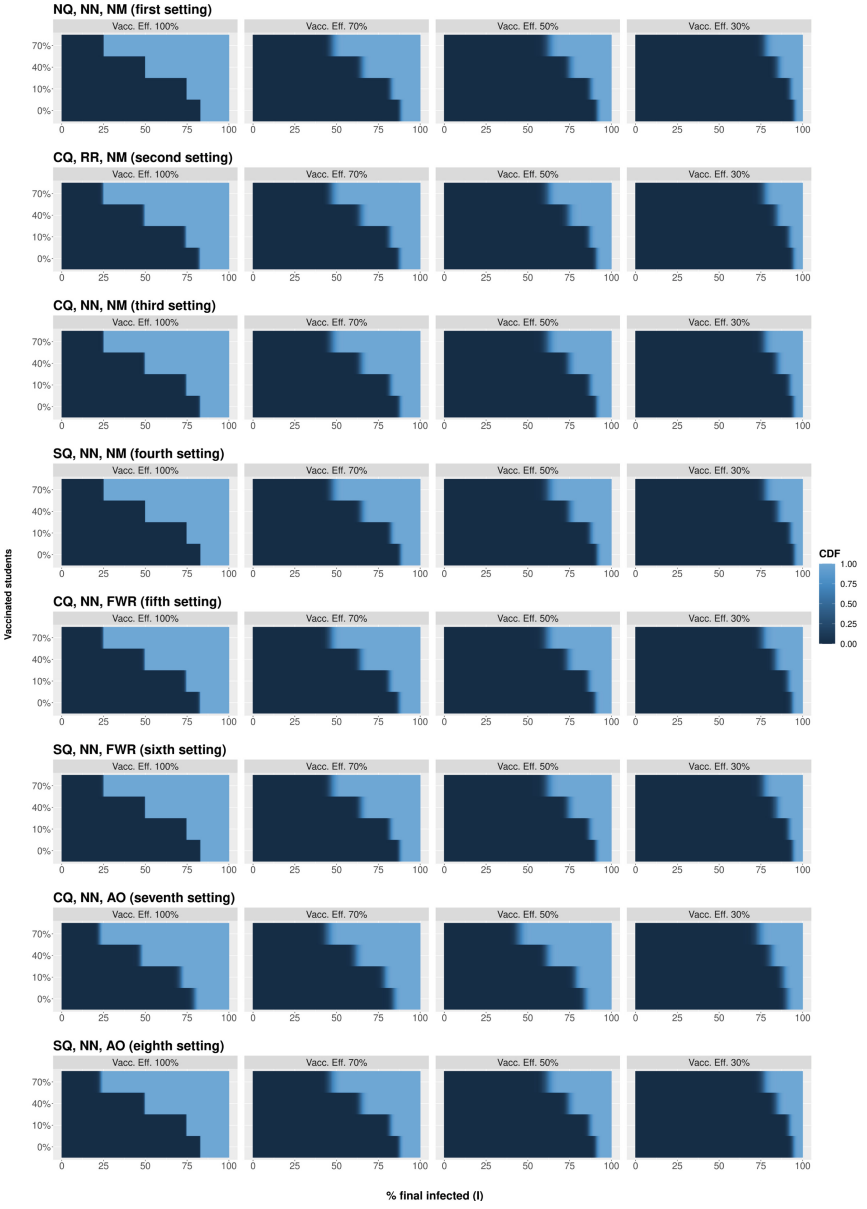

Fig. 5. Cumulative distribution function (CDF) of the total number of infected agents at the final time for each considered scenario under a high virus circulation level. For each scenario—identified by the setting (on the rows), the vaccine efficacy (on the columns), and the fraction of vaccinated students (on the rows of each subplot)—we run 500 simulations—see Table 2. Lighter CDFs indicate more effective countermeasures. We can state that higher infections are associated with lower vaccine efficacies and lower fractions of vaccinated students and a combination of masks and quarantine policies allows to reduce the final number of infected agents.

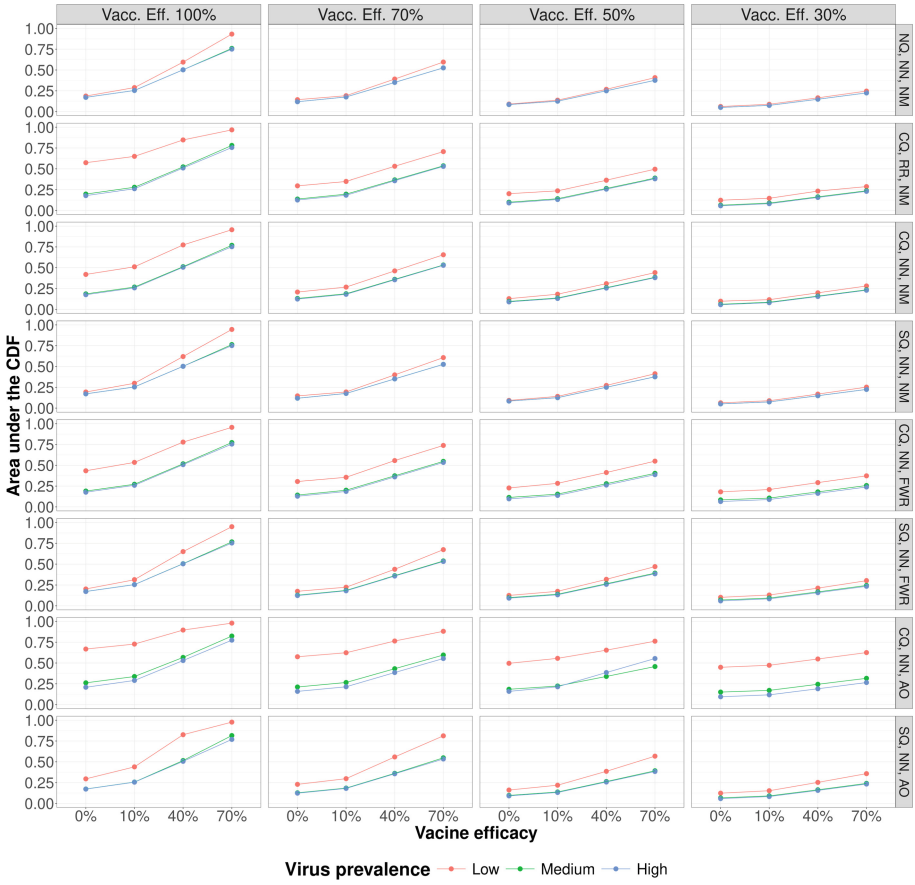

Fig. 6. Area under the CDFs—normalized between 0 and 1—showed in Fig. 3—low virus circulation, in red—, Fig. 4—medium virus circulation, in green—, and Fig. 5—high virus circulation, in blue. For each scenario—identified by the setting (on the rows), the vaccine efficacy (on the columns), the fraction of vaccinated students (on the columns of each subplot), and the virus circulation level (distinguished by the colors)—, the values represent the effectiveness of the implemented countermeasures in the considered scenario. Higher values indicate greater effectiveness of the countermeasures. Virus prevalence appears to influence the area under the CDF differently across the scenarios, with low prevalence often having higher values compared to medium and high prevalence, particularly in scenarios with higher vaccine efficacy.

spread of the infection and, more significantly, how they shift the probability of a negative outcome towards a more convenient one in the presence of different probability masses. In particular, Fig. 7a clearly shows two main outcomes under a low virus circulation level: the infection fades or explodes in a major outbreak. Such behavior is easily observed in the violin plot, where the probability mass gets either at zero or between the susceptible population size and half of the sus-

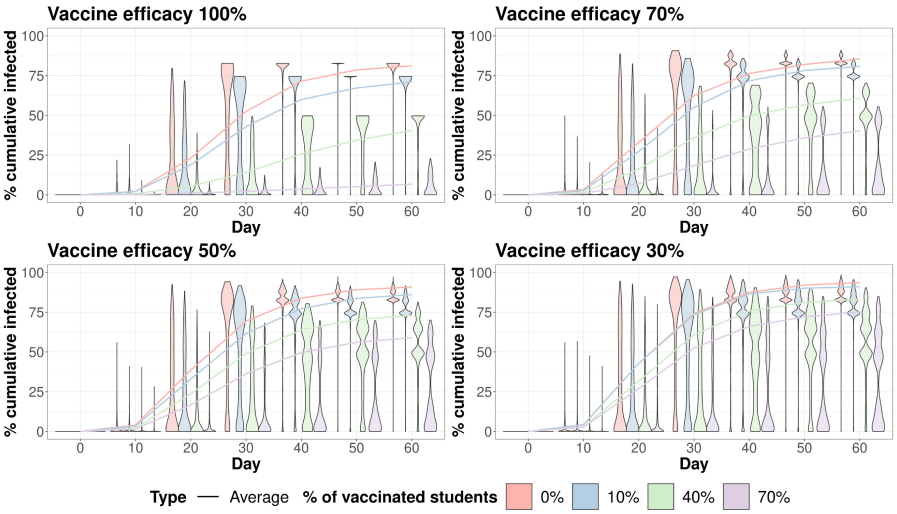

(a) First setting (NQ, NN, NM). Various probability masses emerge with two main outcomes: the infection fades or explodes in a major outbreak.

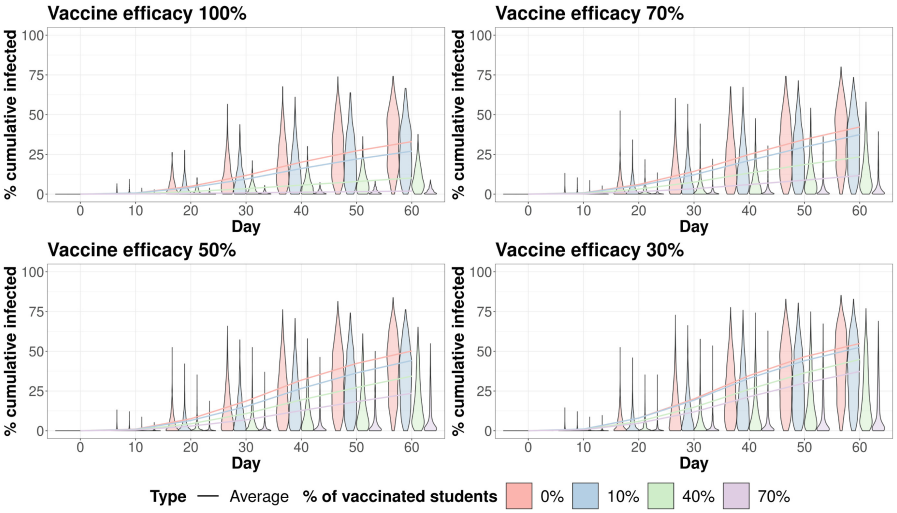

(b) Seventh setting (CQ, NN, AO). The outcome leading to a major outbreak is no longer present: masks and quarantine slow down the infection and contain the risk of a major outbreak.

Fig. 7. Distributions of infections over time and the average number of infections for each considered scenario in the first and seventh settings under a low virus circulation level. For each scenario—the sub-figures illustrate two distinct settings, with each subplot representing a different vaccine efficacy level and the varying colors in each subplot correspond to different fractions of vaccinated students—we run 500 simulations—see Table 2.

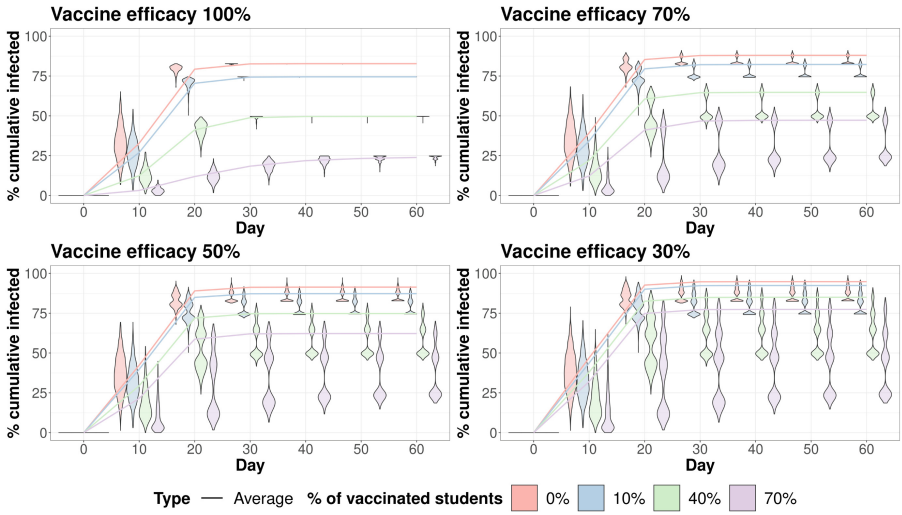

(a) First setting (NQ, NN, NM).

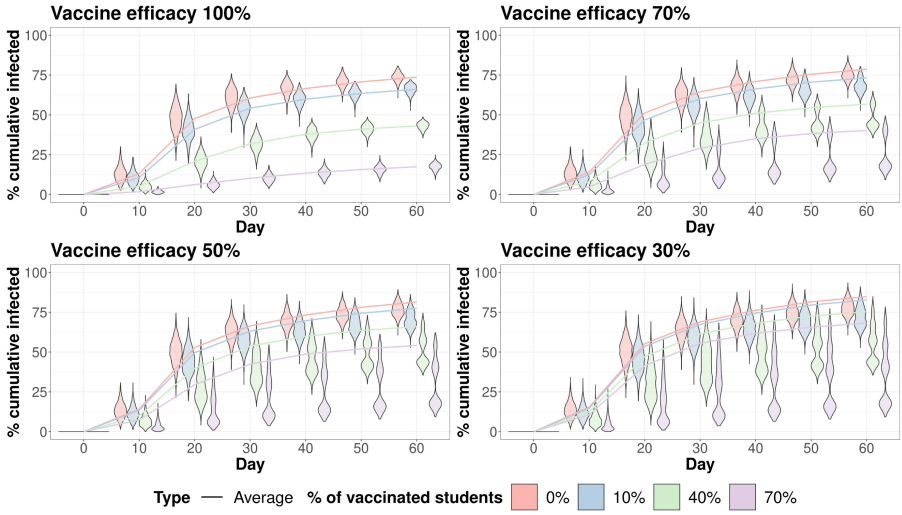

(b) Seventh setting (CQ, NN, AO).

Fig. 8. Distributions of infections over time and the average number of infections for each considered scenario in the first and seventh settings under a medium virus circulation level. For each scenario—the sub-figures illustrate two distinct settings, with each subplot representing a different vaccine efficacy level and the varying colors in each subplot correspond to different fractions of vaccinated students—we run 500 simulations—see Table 2. The vanishing of the infection is no longer present and different probability masses emerged. The most favorable outcome is represented by the probability mass with the lowest mean. A combination of masks and quarantine policies allows to reduce the final number of infections.

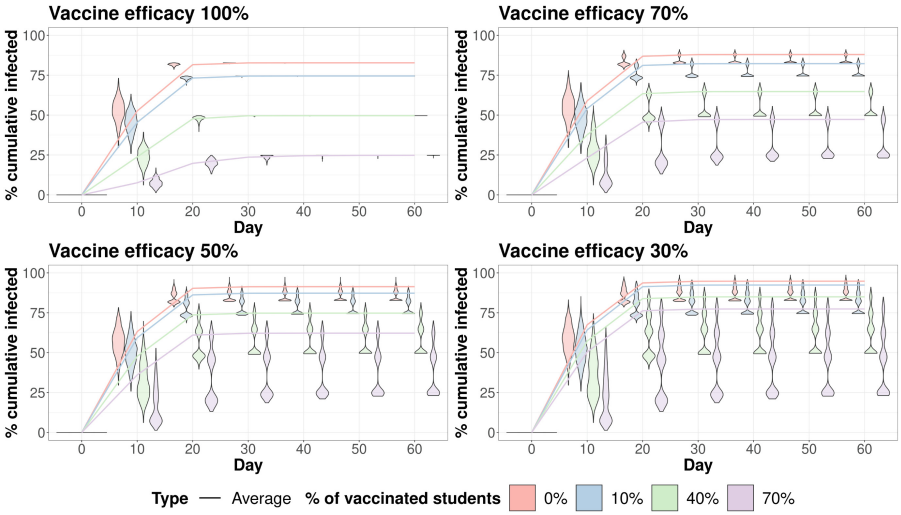

(a) First setting (NQ, NN, NM).

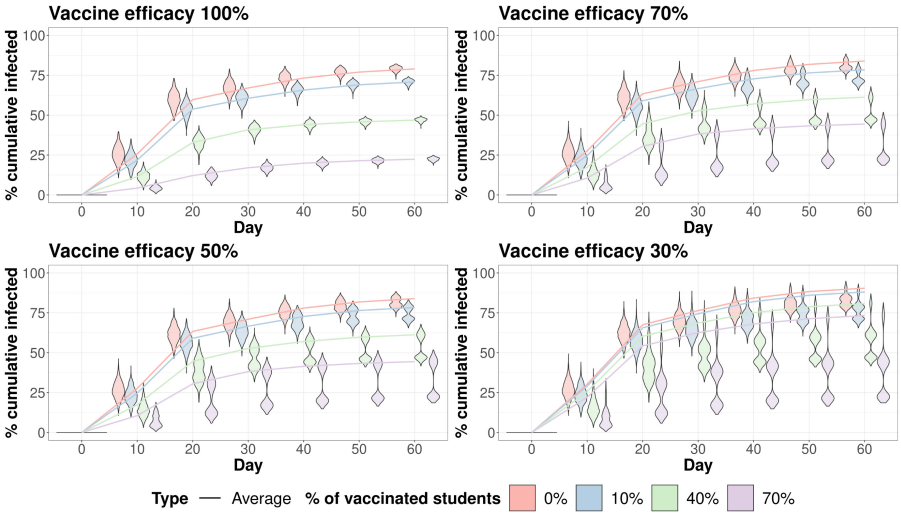

(b) Seventh setting (CQ, NN, AO).

Fig. 9. Distributions of infections over time and the average number of infections for each considered scenario in the first and seventh settings under a high virus circulation level. For each scenario—the sub-figures illustrate two distinct settings, with each subplot representing a different vaccine efficacy level and the varying colors in each subplot correspond to different fractions of vaccinated students—we run 500 simulations—see Table 2. The vanishing of the infection is no longer present and different probability masses emerged. The most favorable outcome is represented by the probability mass with the lowest mean. A combination of masks and quarantine policies allows to reduce the final number of infections.

ceptible population size—intended as the number of agents not covered by the vaccine immunity. The impact of introducing the AO mask policy and the CQ quarantine policy is clear when we consider Fig. 7b. Indeed, here the probability mass is shifted towards a lower number of infections at each time point. Also, the outcome leading to a major outbreak is not present anymore. This result clearly shows the efficacy of the NPIs countermeasure: although masks and quarantine are not enough to stop the spread of the infection they allow to slow it down and contain, if not avoid, the risk of a major outbreak under a low virus circulation level.

Figures 8a, 8b, 9a and 9b show the possible outcomes under a medium and high virus circulation level. In particular, it is straightforward that the best outcome, i.e., the vanishing of the infection, is no longer present. With a vaccine efficacy less or equal to 70% different probability masses emerge from the results. In particular, the best outcome is represented by the probability mass with the lowest mean. From these figures, it is clear that a combination of masks and quarantine policies allow to reduce the final number of infections. Specifically, the CQ quarantine policy and the AO mask policy represent the best outcome also under a medium and high virus circulation level. More generally, even if we no longer have the extinction of the infection, the use of NPIs makes it possible to slow down its spread. We can conclude by observing that NPIs are effective when they manage to outrun the infection, which is why increasing virus circulation decreases effectiveness.

4 Conclusion

We developed an ABM [15] to study the evolution of SARS-CoV-2 spread in a school. We used this model to showcase different NPI approaches to contain the spreading of the virus. Specifically, we considered a baseline setting where no interventions are implemented. That allows us to better understand what happens when NPIs are introduced. In particular, we compared the effects of wearing masks all the time and the implementation of a testing protocol, using two quarantine policies used in the Piedmont region of Italy in 2021 and 2022.

The computational modeling allowed us to pinpoint several useful takeaways for policymakers. First of all, vaccination campaigns covering less than 40% of the susceptible population provide poor results in protecting from a major outbreak. Furthermore, we showed that testing campaigns are effective as far as the testing process is faster than the virus diffusion. On the other hand, wearing masks properly is an effective countermeasure also when the infection speeds up.

Eventually, the introduction of an infection external to the school allows us to consider different settings of infection prevalence—where in this work we consider three different levels of infection's prevalence in the general population. In particular, in a setting with a medium or high circulation of the virus, the results show that it is more challenging to contain the spread for a low virus circulation level, but a combination of masks and quarantine policies allows to reduce the final number of infections.

NPIs are useful for infection, especially in the early stages and can help to keep activities open even in scenarios with higher circulation, but they must be supported by other public health instruments.

Acknowledgments. DB is a Ph.D. student enrolled in the National Ph.D. in Artificial Intelligence, XXXVII cycle, course on health and life sciences, organized by Università Campus Bio-Medico di Roma.

Funding Information. This work was supported by grants from "Creation of a computational framework to model and study West Nile Disease" (Cod. ROL 67410, PI Marco Beccuti), and "Ripresa delle attività socio-economiche e delle scuole: modelli per la progettazione e supporto di linee guida per la convivenza con il Covid-19" (Cod. ROL 73459, 2020, PI Matteo Sereno), projects funded by CRT foundation. This work is part of the project TrustAlert which has received funding from the Fondazione Compagnia San Paolo and Fondazione CDP under the "Artificial Intelligence" call.

Conflict of interests. All authors declare that they have no conflicts of interest.

Availability of data and software code. The ABM developed for the analysis presented in this work and the configurations presented above are available at https://github.com/qBioTurin/epischool-abm/tree/CIBB.

References

1. Eales, O., et al.: Dynamics of competing SARS-CoV-2 variants during the Omicron epidemic in England. Nat. Commun. **13**(1), 4375 (2022)
2. Watson, O.J., Barnsley, G., Toor, J., Hogan, A.B., Winskill, P., Ghani, A.C.: Global impact of the first year of COVID-19 vaccination: a mathematical modelling study. Lancet Infect. Dis. **22**(9), 1293–1302 (2022)
3. Perra, N.: Non-pharmaceutical interventions during the COVID-19 pandemic: a review. Phys. Rep. **913**, 1–52 (2021)
4. Pernice, S., et al.: Impacts of reopening strategies for COVID-19 epidemic: a modeling study in Piedmont region. BMC Infect. Dis. **20**, 1–9 (2020)
5. Wells, C.R., et al.: Optimal COVID-19 quarantine and testing strategies. Nat. Commun. **12**(1), 356 (2021)
6. Villers, J., et al.: SARS-CoV-2 aerosol transmission in schools: the effectiveness of different interventions. Swiss Med. Wkly, **152**(2122), w30178 (2022)
7. Gkantonas, S., Zabotti, D., Mesquita, L.C.C., Mastorakos, E., de Oliveira, P.M.: airborne. cam: a risk calculator of SARS-CoV-2 aerosol transmission under well-mixed ventilation conditions (2021)
8. Kerr, C.C., et al.: Covasim: an agent-based model of COVID-19 dynamics and interventions. PLOS Comput. Biol. **17**(7), e1009149 (2021)
9. Woodhouse, M.J., Aspinall, W.P., Sparks, R., Brooks-Pollock, E., Relton, C.: Alternative Covid-19 mitigation measures in school classrooms: analysis using an agent-based model of SARS-CoV-2 transmission. Roy. Soc. Open Sci. **9**(8), 211985 (2022)
10. Fouad, A.A., Antably, A.E.: Agent-based modeling and simulation of pandemic propagation in a school environment. Int. J. Architectural Comput. **21**(1), 120–135 (2023)

11. Faucher, B., et al.: Agent-based modelling of reactive vaccination of workplaces and schools against COVID-19. Nat. Commun. **13**(1), 1414 (2022)
12. Lasser, J., Sorger, J., Richter, L., Thurner, S., Schmid, D., Klimek, P.: Assessing the impact of SARS-CoV-2 prevention measures in Austrian schools using agent-based simulations and cluster tracing data. Nat. Commun. **13**(1), 554 (2022)
13. Lorig, F., Johansson, E., Davidsson, P.: Agent-based social simulation of the Covid-19 pandemic: a systematic review. J. Artif. Soc. Soc. Simul. **24**(3), 5 (2021)
14. Tatapudi, H., Das, T.K.: Impact of school reopening on pandemic spread: a case study using an agent-based model for COVID-19. Infect. Dis. Model. **6**, 839–847 (2021)
15. Baccega, D., et al.: An agent-based model to support infection control strategies at school. J. Artif. Soc. Soc. Simul. **25**(3), 2 (2022)
16. Uri Wilensky. NetLogo (1999). http://ccl.northwestern.edu/netlogo/
17. Hoertel, N., et al.: A stochastic agent-based model of the SARS-CoV-2 epidemic in France. Nat. Med. **26**(9), 1417–1421 (2020)
18. Buonanno, G., Stabile, L., Morawska, L.: Estimation of airborne viral emission: quanta emission rate of SARS-CoV-2 for infection risk assessment. Environ. Int. **141**, 105794 (2020)
19. Watanabe, T., Bartrand, T.A., Weir, M.H., Omura, T., Haas, C.N.: Development of a dose-response model for SARS coronavirus. Risk Anal. Int. J. **30**(7), 1129–1138 (2010)
20. Peng, Z., et al.: Practical indicators for risk of airborne transmission in shared indoor environments and their application to COVID-19 outbreaks. Environ. Sci. Technol. **56**(2), 1125–1137 (2022)
21. Baccini, M., Cereda, G.: Screening plans for SARS-CoV-2 based on sampling and rotation: an example in a European school setting. PLOS ONE **16**(9), 1–13 (2021)
22. Piemonte, R.: Scuola: operative entro il 17 novembre le nuove regole per le quarantene. https://www.regione.piemonte.it/web/pinforma/notizie/scuola-operative-entro-17-novembre-nuove-regole-per-quarantene
23. Zaki, N., Mohamed, E.A.: The estimations of the COVID-19 incubation period: a scoping reviews of the literature. J. Infect. Public Health **14**(5), 638–646 (2021)
24. World Health Organization. Coronavirus disease 2019 (COVID-19): situation report, 73. Technical documents (2020)
25. Byrne, A.W., et al.: Inferred duration of infectious period of SARS-CoV-2: rapid scoping review and analysis of available evidence for asymptomatic and symptomatic COVID-19 cases. BMJ Open, **10**(8) (2020)